PERGAMON International Journal of Multiphase Flow 24 (1998) 793–824

International Journal of Multiphase Flow

Electrophoretic motion of a charged spherical particle normal to a planar dielectric wall

Y. Hao, S. Haber *

Department of Mechanical Engineering, Technion-Israel Institute of Technology, Haifa, Israel

Received 13 November 1996; received in revised form 25 November 1997

Abstract

The electrophoretic motion of a charged spherical particle perpendicular to a single planar dielectric wall or that between a perfectly conducting wall and a dielectric wall is analytically studied. Particle velocity is determined by a rectified Smoluchowski's velocity that accounts for wall effects. Parameters affecting particle velocity are the direction of the applied electric field, the ratio between the particle and the wall zeta potentials, the ratio between particle diameter and its center distance to the walls, the ratio between the dielectric constants of the fluid and that of the dielectric wall and the ratio between the thickness of the dielectric layer and its distance to the particle center.

Two competing mechanisms govern the overall wall effect that charged particles experience. The first mechanism (explored in detail) stems from the drag force induced by the electroosmotic flow that is generated near the dielectric wall. It may cause either particle velocity retardation or enhancement. Velocity retardation is obtained for negative values of wall to particle zeta potential ratios and a velocity increase for positive ratios. Thus, a positively charged particle moving *toward* the dielectric wall experiences a velocity increase when the wall zeta potential is positive, and a velocity retardation for negative wall zeta potentials. The second mechanism is a purely hydrodynamic wall effect. It causes particles that move perpendicular to the wall to experience a velocity retardation regardless of their direction of motion.

Keywords: Electrophoretic motion; Spherical particles; Dielectric wall effects

1. Introduction

The electrophoretic motion of a charged particle in externally bounded electrolyte solution is of considerable interest in a wide range of applications such as, electrodeposition of paint

* To whom correspondence should be addressed.

0301-9322/98/$19.00
PII: S0301-9322(97)00090-6

(EDP) or electrocoating, an electrophoretic process in which the charged colloidal particles are dispersed in solution and deposited on electrodes under the influence of an electric field (Beck, 1981). The electrophoretic velocity of a charged particle suspended in an unbounded field is given by Smoluchowski's equation (Probstein, 1994; Morrison, 1970; Hunter, 1981),

$$U_{\mathrm{p}} = \frac{\varepsilon \zeta_{\mathrm{p}}}{4\pi\mu} E_{\infty}, \tag{1}$$

provided that the thickness of the electrical double layer (the Debye length) is everywhere small compared with particle dimension. Here ε is the electrolyte solution permittivity, ζ_{p} the Zeta potential of the particle surface, μ the fluid viscosity, and E_{∞} the applied electric field.

The presence of neighbouring particles or rigid boundaries close to the charged particle lead to corrections of Smoluchowski's equation. The case in which an insulting sphere approaches a planar conducting wall in a uniform electric field was treated by Morrison and Stukel (1970) using bipolar coordinates. Keh and Anderson (1985) investigated the same problem by using the method of reflections and obtained an approximate solution for the electrophoretic velocity of charged particles. Similarly, "exact" and asymptotic solutions for the electrophoretic velocity of an insulated sphere moving parallel to an insulated planar wall were derived by Keh and Chen (1988) and Keh and Anderson (1985) utilizing the two above-mentioned methods.

Keh and Jan (1996) took into account the polarization of the diffuse species in the thin particle-solute interaction layer for a colloidal sphere moving toward a planar wall.

Reed and Morrison (1976) studied the electrophoretic motions of two dielectric spheres applying the spherical bipolar coordinates. Analysis of the same problem was presented by Chen and Keh (1988) using the method of reflections.

Keh and Anderson (1985) suggested that the following boundary conditions prevail over the enveloping surface of a particle and near a rigid wall bounding the fluid.

On a particle surface

$$\mathbf{n} \cdot \nabla \phi = 0, \tag{2}$$

$$\mathbf{v} = \mathbf{U} + \Omega \times \mathbf{r} + \frac{\varepsilon \zeta_{\mathrm{p}}}{4\pi\mu} (\mathbf{I} - \mathbf{nn}) \cdot \nabla \phi, \tag{3}$$

and on a stationary boundary surface

$$\mathbf{n} \cdot \nabla \phi = 0 \text{ (insulated wall)}, \tag{4a}$$

or

$$\phi = \text{Constant (conducting wall)}, \tag{4b}$$

and

$$\mathbf{v} = \frac{\varepsilon \zeta_{\mathrm{w}}}{4\pi\mu} (\mathbf{I} - \mathbf{nn}) \cdot \nabla \phi, \tag{5}$$

where ϕ is the electric potential, $\mathbf{v}$ the flow velocity, $\mathbf{r}$ the position vector. $\mathbf{I}$ the idem dyadic, $\mathbf{n}$

the unit vector normal to the surface, and **U** and **Ω** are the translational and angular velocity of the particle, respectively.

In previous analyses, Morrison and Stukel (1970) and Keh and Anderson (1985) assumed that the bounding wall is a perfect conductor. In many applications, however, that assumption is invalid. For example, in the color printing industry, the reverse roll coating process employs two parallel coating rolls that rotate with a fixed speed ratio. Between the rolls a very narrow gap is maintained (the nip region). The coating electrolytic fluid is driven into the nip region between the rolls by the applicator where it separates with one layer transferred to the backward rotating roll and the other passing through the nip region to form the metering film. Small charged particles, the pigments, embedded in the electrolytic fluid migrate driven by a strong electric field. The field is applied between the perfectly conducting wall of the applicator roll (the anode) and the backward rotating roll (the cathode) that is coated with a thin dielectric layer. The printed matrix quality depends mainly on the lateral motion of the pigments between the rolls and their deposition sites on the dielectric layer.

Normally, the order of magnitude of the diameter of the rolls is tens of centimeters and that of the minimum gap between them is tens of micrometers. The thickness of the dielectric layer and the particles diameter is of the order of micrometers. Thus, a geometrical model consisting a spherical particle between planar walls provides a good approximation of the system configuration. In addition, the inclusion of the dielectric layer in our model not only mimics the actual configuration of the system, but it also adds a new electroosmotic effect to the hydrodynamic and electrophoretic mechanisms that govern particle lateral motion. It is the goal of this paper to analyze the different mechanisms governing particle motion and their relative significance. In this context, we consider in Section 2 the case of a sphere moving near a dielectric planar wall in an otherwise unbounded fluid. In Section 3, the perpendicular electrophoretic motion of a particle between a conducting plane and a dielectric planar wall is analyzed.

2. The electrophoretic motion of a particle perpendicular to a single dielectric wall

Consider the electrophoretic motion of a charged insulated spherical particle of radius a perpendicular to an infinite conducting plane wall covered with dielectric of thickness t. The particle center is located at a distance b from the wall (Fig. 1). Polar (ρ, Φ, z) or spherical (r, Φ, θ) coordinates are used with the origin located at the sphere center. All of the Φ-dependent terms vanish in the subsequent analysis due to axisymmetry.

In this problem an electrophoretic flow field is induced by the electric field. Therefore, in order to characterize the particle's electrophoretic motion, the electric field about the particle must be determined first.

2.1. Assumptions

To capture the main effects characterizing particle motion, the following simplifying assumptions are made:

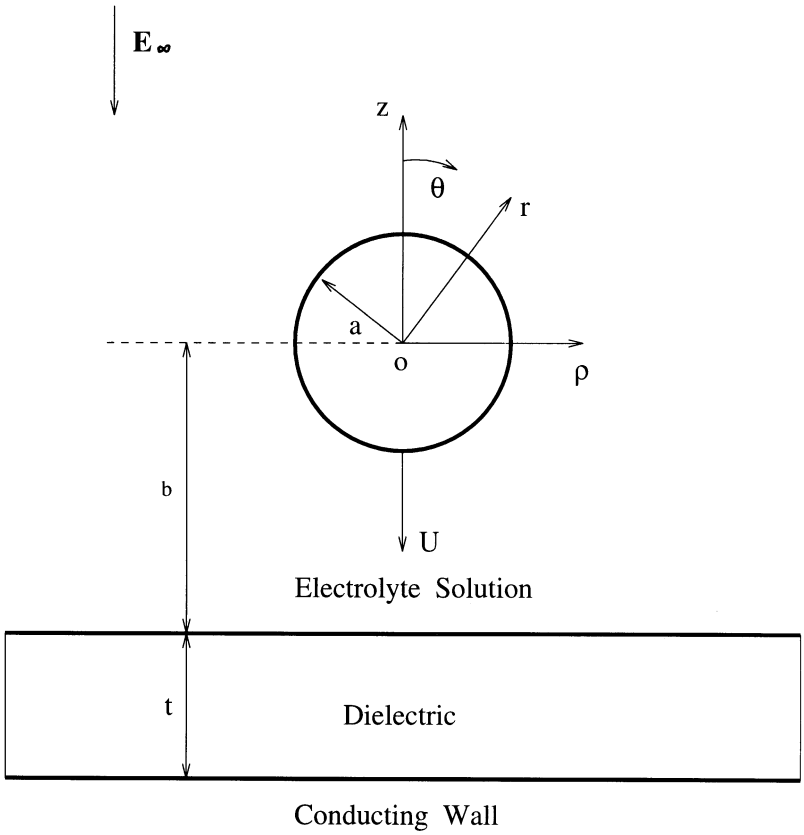

Fig. 1. The electrophoretic system configuration.

- The fluid is Newtonian;
- The flow is quasi-steady and creeping (namely, a very low Reynolds number flow);
- The particle is rigid and perfectly insulated. Both the particle and the planar wall surfaces are assumed to be uniformly charged;
- The radius of the particle is much larger than the thickness of the electric double layer, say the Debye thickness;
- Far from the particle, the applied electric field acting perpendicular to the plane wall is uniform;
- The fluid outside the double layer is neutral and is assumed to be of constant conductivity.
- The applied electric potential is much larger than the zeta potentials that develop over the sphere and the dielectric plane.

2.2. Governing equation and boundary conditions for the electric field

The governing equations for the electric potential distributions ϕ and ϕ_w inside the electrolyte and the dielectric layer, respectively, satisfy Laplace's equation (Morrison, 1970;

Probstein, 1994):

$$\nabla^2\phi = 0 \ @ \ -b \le z < \infty, \tag{6}$$

$$\nabla^2\phi_w = 0 \ @ \ -(b+t) \le z < -b. \tag{7}$$

Equations (6) and (7) with the appropriate boundary conditions will be solved by the method of reflections. The electric field, far from the particle, is supposed to be of uniform strength E_∞, and directed along the z-axis. The wall beneath the dielectric ($z < -b-t$) is perfectly conducting. On the interface between the electrolyte solution and the dielectric layer, Gauss' law for electric field densities must be observed (Haus and Melcher, 1989). Thus the potential ϕ is continuous and $\varepsilon(\mathbf{n}\cdot\nabla\phi) = \varepsilon_w(\mathbf{n}\cdot\nabla\phi_w)$ is satisfied at the interface. Here, ε and ε_w are permittivities of electrolyte solution and dielectric, respectively. Consequently, the boundary conditions for the electric potential can be posed as:

$$\mathbf{n}\cdot\nabla\phi = 0 \text{ at } r = a. \tag{8}$$

$$\phi_w = C \quad \text{at} \quad z = -(b+t), \tag{9}$$

$$\left.\begin{array}{c}\phi = \phi_w \\ \kappa(\mathbf{n}\cdot\nabla\phi) = \mathbf{n}\cdot\nabla\phi_w\end{array}\right\} \quad \text{at} \quad z = -b, \tag{10}$$

$$\phi \longrightarrow -E_\infty z \quad \text{as} \quad z \longrightarrow \infty, \tag{11}$$

where $\kappa = \varepsilon/\varepsilon_w$ and C is a constant.

2.3. Reflections of electric potential ϕ

In the following, a reflection method of solution (Happel and Brenner, 1983) is adopted. Odd reflections satisfy boundary conditions over the planar walls and assume that the fluid occupies the whole volume above the plane $z = -b$. Even reflections satisfy boundary conditions over the sphere surface and assume that the fluid occupies the unbounded volume external to the sphere.

2.3.1. First reflections $\phi^{(1)}$, $\phi_w^{(1)}$

The first reflections of the electric potential $\phi^{(1)}$ and $\phi_w^{(1)}$ satisfy (6) and (7), are subjected to boundary conditions (9)–(11) and assume absence of the particle.

The solutions inside the electrolyte:

$$\phi^{(1)} = -E_\infty z + C_1 \quad -b \le z < \infty, \tag{12}$$

and inside the dielectric

$$\phi_w^{(1)} = -E_\infty\kappa(z+b) + E_\infty b + C_1 \quad -(b+t) \le z \le -b, \tag{13}$$

are straightforward. From (13) and (9) we obtain

$$C = E_\infty b(1 + \kappa\beta) + C_1,$$

where $\beta = t/b$. Since the additive constant C does not affect the final results, we shall henceforth assume that $\phi = 0$ at $z = -(b + t)$. Consequently

$$C_1 = -E_\infty b(1 + \kappa\beta). \tag{14}$$

2.3.2. Second reflection $\phi^{(2)}$

The second reflection of the electric potential $\phi^{(2)}$ satisfies equation (6) and is subjected to the following boundary conditions:

$$\mathbf{n} \cdot \nabla\phi^{(2)} = -\mathbf{n} \cdot \nabla\phi^{(1)} \ @ \ r = a, \tag{15}$$

$$\phi^{(2)} = 0 \ @ \ r \to \infty. \tag{16}$$

Note that in this case the bounding walls are removed. The general solution of the harmonic equation (6) in spherical coordinates is (Lamb, 1932):

$$\phi^{(2)} = \sum_{n=0}^{\infty} A_n r^{-n-1} P_n(\cos\theta), \tag{17}$$

where θ is the latitude angle and P_n are the Legendre polynomials of order n. Obviously, ϕ is independent of the azimuthal angle due to axisymmetry of the problem and only terms that decay at infinity are included. Applying (12) and (15), and the orthogonality of the Legendre polynomials yields

$$A_n = \begin{cases} -\frac{1}{2} E_\infty a^3 & n = 1 \\ 0 & n \neq 1 \end{cases}.$$

Thus, the exact solution of $\phi^{(2)}$ is:

$$\begin{aligned} \phi^{(2)} &= -\frac{1}{2} E_\infty \frac{a^3}{r^2} \cos\theta \\ &= -\frac{1}{2} E_\infty a^3 \frac{z}{(\rho^2 + z^2)^{3/2}}. \end{aligned} \tag{18}$$

2.3.3. Third reflections $\phi^{(3)}$, $\phi_w^{(3)}$

The third reflection of the electric potentials $\phi^{(3)}$ and $\phi_{\mathrm{w}}^{(3)}$ satisfy the harmonic equations:

$$\nabla^2\phi^{(3)} = 0, \tag{19}$$

$$\nabla^2\phi_{\mathrm{w}}^{(3)} = 0, \tag{20}$$

and the boundary conditions:

$$\phi_{\mathrm{w}}^{(3)} = -\phi^{(2)} = -\frac{E_\infty a^3}{2}\frac{(b+t)}{[\rho^2+(b+t)^2]^{3/2}} \ @\ z=-(b+t), \tag{21}$$

$$\phi^{(3)} = \phi_{\mathrm{w}}^{(3)} \ @\ z=-b, \tag{22a}$$

$$\kappa[\mathbf{n}\cdot\nabla\phi^{(3)}] - [\mathbf{n}\cdot\nabla\phi_{\mathrm{w}}^{(3)}] = -(\kappa-1)[\mathbf{n}\cdot\nabla\phi^{(2)}] \ @\ z=-b, \tag{22b}$$

$$\phi^{(3)} = 0 \ @\ z\to\infty. \tag{23}$$

Applying the Hankel transform (Sneddon, 1951),

$$\Phi(\xi,z) = \int_0^\infty \rho\phi(\rho,z)J_0(\rho\xi)\,\mathrm{d}\rho,$$

(19) rewritten in cylindrical coordinates results in:

$$\frac{\mathrm{d}^2\Phi}{\mathrm{d}z^2} - \xi^2\Phi = 0. \tag{24}$$

The inverse Hankel transform is:

$$\phi(\rho,z) = \int_0^\infty \xi\Phi(\xi,z)J_0(\rho\xi)\,\mathrm{d}\xi,$$

where J_0 is the Bessel function of zero order and ξ a dummy variable. The general solution of (24) that decays at infinity is:

$$\Phi(\xi,z) = A(\xi)\mathrm{e}^{-\xi(z+b)},$$

where A(ξ) is an unknown function of ξ. Consequently, the inverse transform yields,

$$\phi(\rho,z) = \int_0^\infty A(\xi)\mathrm{e}^{-\xi(z+b)}\xi J_0(\rho\xi)\,\mathrm{d}\xi. \tag{25}$$

Similarly, the transformed electric potential $\phi_{\mathrm{w}}^{(3)}$ satisfies the equation,

$$\frac{\mathrm{d}^2\Phi_{\mathrm{w}}}{\mathrm{d}z^2} - \xi^2\Phi_{\mathrm{w}} = 0,$$

that possesses the following general solution:

$$\Phi_{\mathrm{w}}(\xi,z) = B(\xi)\sinh[\xi(z+b)] + C(\xi)\cosh[\xi(z+b)],$$

where B(ξ) and $C(\xi)$ are yet to be determined functions of ξ. From Gradshteyn and Ryzhik (1994), boundary condition (21) can be expressed as

$$-B(\xi)\sinh(\xi t)+C(\xi)\cosh(\xi t)=-\frac{E_\infty a^3}{2}\int_0^\infty \frac{b+t}{[\rho^2+(b+t)^2]^{3/2}}\rho J_0(\rho\xi)\,\mathrm{d}\rho$$

$$=-\frac{E_\infty a^3}{2}\mathrm{e}^{-(b+t)\xi}. \tag{26}$$

Hence, the general solution of (20) is given by the inverse transformation

$$\phi_{\mathrm{w}}(\rho,z)=\int_0^\infty\{\left[C(\xi)\frac{\cosh(\xi t)}{\sinh(\xi t)}+\frac{E_\infty a^3}{2}\frac{\mathrm{e}^{-(b+t)\xi}}{\sinh(\xi t)}\right]\sinh[\xi(z+b)]$$

$$+C(\xi)\cosh[\xi(z+b)]\}\xi J_0(\rho\xi)\,\mathrm{d}\xi. \tag{27}$$

Substituting (25) and (27) into boundary conditions (22) yields two algebraic equations for the two unknown functions $A(\xi)$ and $C(\xi)$,

$$A(\xi)=C(\xi), \tag{28}$$

$$-\kappa A(\xi)-C(\xi)\frac{\cosh(\xi t)}{\sinh(\xi t)}-\frac{E_\infty a^3}{2}\frac{\mathrm{e}^{-(b+t)\xi}}{\sinh(\xi t)}=(1-\kappa)\frac{E_\infty a^3}{2}\mathrm{e}^{-b\xi}. \tag{29}$$

Finally, solving (28), (29) and using (26) results in

$$A(\xi)=-\frac{E_\infty a^3}{2}\mathrm{e}^{-b\xi}\frac{\cosh(\xi t)-\kappa\sinh(\xi t)}{\cosh(\xi t)+\kappa\sinh(\xi t)},$$

$$B(\xi)=-\frac{E_\infty a^3}{2}\mathrm{e}^{-b\xi}\frac{\cosh(\xi t)-\kappa\sinh(\xi t)+2\kappa\mathrm{e}^{-\xi t}}{\cosh(\xi t)+\kappa\sinh(\xi t)}, \tag{30}$$

$$C(\xi)=-\frac{E_\infty a^3}{2}\mathrm{e}^{-b\xi}\frac{\cosh(\xi t)-\kappa\sinh(\xi t)}{\cosh(\xi t)+\kappa\sinh(\xi t)}.$$

Consequently, the exact solution of the third reflection possesses the integral solution form

$$\phi^{(3)}=-\frac{E_\infty a^3}{2}\int_0^\infty\frac{\cosh(\xi t)-\kappa\sinh(\xi t)}{\cosh(\xi t)+\kappa\sinh(\xi t)}\mathrm{e}^{-(z+2b)\xi}\xi J_0(\rho\xi)\,\mathrm{d}\xi, \tag{31}$$

$$\phi_{\mathrm{w}}^{(3)}=\frac{E_\infty a^3}{2}\left[\int_0^\infty\frac{(\kappa-1)\cosh(\xi t)}{\cosh(\xi t)+\kappa\sinh(\xi t)}\mathrm{e}^{\xi z}\xi J_0(\rho\xi)\,\mathrm{d}\xi\right.$$
$$\left.-\int_0^\infty\frac{\kappa\mathrm{e}^{-\xi t}}{\cosh(\xi t)+\kappa\sinh(\xi t)}\mathrm{e}^{-(z+2b)\xi}\xi J_0(\rho\xi)\,\mathrm{d}\xi\right] \tag{32}$$

2.3.4. Fourth reflection $\gamma^{(4)}$

The fourth reflection satisfies the boundary conditions over the surface of a sphere embedded in an unbounded field,

$$\mathbf{n}\cdot\nabla\phi^{(4)} = -\mathbf{n}\cdot\nabla\phi^{(3)} \ @\ r = a, \tag{33}$$

$$\phi^{(4)} = 0 \ @\ r\to\infty. \tag{34}$$

An approximate solution of (6) in terms of spherical coordinates is given by Keh and Anderson (1985):

$$\phi^{(4)} = \frac{1}{2}\frac{a^3}{r^2}\left[\frac{\partial\phi^{(3)}}{\partial r}\right]|_{r=0} + \frac{1}{3}\frac{a^5}{r^3}\left[\frac{\partial^2\phi^{(3)}}{\partial r^2}\right]|_{r=0} + \frac{1}{8}\frac{a^7}{r^4}\left[\frac{\partial^3\phi^{(3)}}{\partial r^3}\right]|_{r=0} + \ldots. \tag{35}$$

Substituting (31) into (35) yields,

$$\phi^{(4)} = \frac{E_\infty a^3}{4}\left[\frac{\lambda^3}{r^2}\cos\theta\left(\frac{1}{4} - I_1\right) + \frac{1}{3}\frac{a\lambda^4}{r^3}\left(\frac{3}{8} - I_2\right)(\sin^2\theta - 2\cos^2\theta)\right] + \mathrm{o}(a^5\lambda^5), \tag{36}$$

where

$$\lambda = \frac{a}{b},$$

$$I_1 = \int_0^\infty \frac{2\kappa\sinh(\xi\beta)}{\cosh(\xi\beta) + \kappa\sinh(\xi\beta)}\xi^2 e^{-2\xi}\,d\xi, \tag{37a}$$

$$I_2 = \int_0^\infty \frac{2\kappa\sinh(\xi\beta)}{\cosh(\xi\beta) + \kappa\sinh(\xi\beta)}\xi^3 e^{-2\xi}\ \ d\xi. \tag{37b}$$

2.3.5. Fifth reflection $\phi^{(5)}$, $\phi_w^{(5)}$

The fifth reflection field satisfies the differential equations

$$\nabla\phi^{(5)} = 0, \tag{38a}$$

$$\nabla\phi_w^{(5)} = 0, \tag{38b}$$

and boundary conditions,

$$\phi_w^{(5)} = -\phi^{(4)} \ @\ z = -(b + t), \tag{39}$$

$$\phi^{(5)} = \phi_w^{(5)} \ @\ z = -b, \tag{40a}$$

$$\kappa[\mathbf{n}\cdot\nabla\phi^{(5)}] - [\mathbf{n}\cdot\nabla\phi_w^{(5)}] = -(\kappa - 1)[\mathbf{n}\cdot\nabla\phi^{(4)}] \ @\ z = -b, \tag{40b}$$

$$\phi^{(5)} = 0 \ @ \ z \to \infty. \tag{41}$$

Applying Hankel transforms to equations (38), and using (36), (39), (40) and (41), we obtain:

$$\phi^{(5)} = \frac{E_\infty a^3}{4} \int_0^\infty \frac{\cosh(\xi t) - \kappa \sinh(\xi t)}{\cosh(\xi t) + \kappa \sinh(\xi t)} [\lambda^3 \left(\frac{1}{4} - I_1\right)$$

$$+ \frac{a\lambda^4}{3} \left(\frac{3}{8} - I_2\right) \xi] \mathrm{e}^{-(z+2b)\xi} J_0(\rho\xi) \xi \mathrm{d}\xi + \mathrm{o}(a\lambda^9), \tag{42}$$

where the solution process is similar to that of the third reflection.

2.3.6. Final electric potential ϕ

The electric potential in the electrolyte solution that is given by the sum,

$$\phi = \phi^{(1)} + \phi^{(2)} + \phi^{(3)} + \phi^{(4)} + \phi^{(5)} + \cdots, \tag{43}$$

represents an approximate solutions of ϕ of $\mathrm{o}(\lambda^9)$. It satisfies exactly the boundary conditions over the planar walls and only approximately those over the sphere surface.

2.4. The flow field equations and boundary conditions

Having obtained a solution for the electric field about the particle, it is now possible to use a similar method of reflections to obtain the flow field. Owing to sufficiently slow motion of the particle, the flow field outside the thin double layer is governed by the Stokes equations,

$$\nabla \cdot \mathbf{v} = 0, \tag{44}$$

$$\mu \nabla^2 \mathbf{v} = \nabla p, \tag{45}$$

where μ is the fluid viscosity and $\mathbf{v}$ and p are the velocity and pressure fields, respectively. According to (3) and (5), the following boundary conditions must be satisfied:

$$\mathbf{v} = \mathbf{U} + \frac{\varepsilon \zeta_\mathrm{p}}{4\pi\mu} \nabla\phi \ @ \ r = a, \tag{46}$$

$$\mathbf{v} = \frac{\varepsilon \zeta_\mathrm{w}}{4\pi\mu} (\mathbf{I} - \mathbf{nn}) \cdot \nabla\phi \ @ \ z = -b, \tag{47}$$

$$\mathbf{v} = 0 \ @ \ z = \infty, \tag{48}$$

where ζ_p and ζ_w are zeta potentials of the particle and the wall, respectively, and $\mathbf{U}$ is the electrophoretic translational velocity of the particle. No angular velocity of the particle is introduced due to axisymmetry of the problem.

The procedure used by Keh and Anderson (1985) for the determination of the flow field and electrophoretic velocity of the particle is adopted here. In the following reflections, the even

reflections are reflected from the particle while the odd reflections are reflected from the wall. The boundary conditions for the even reflected fields can be expressed as:

$$\mathbf{v}^{(i)} = -\mathbf{v}^{(i-1)} + \mathbf{U}^{(i/2)} + \frac{\varepsilon\zeta_{\mathrm{p}}}{4\pi\mu}\nabla[\phi^{(i-1)} + \phi^{(i)}], \tag{49}$$

where $\mathbf{U}^{(\mathrm{i}/2)}$ is related to the $(i-1)$th reflected electric field and flow field from the wall by:

$$\mathbf{U}^{(i/2)} = -\frac{\varepsilon\zeta_{\mathrm{p}}}{4\pi\mu}[\nabla\phi^{(i-1)}]_{\mathrm{o}} + [\mathbf{v}^{(i-1)}]_{\mathrm{o}} + \frac{1}{6}a^2[\nabla^2\mathbf{v}^{(i-1)}]_{\mathrm{o}}, \tag{50}$$

where subscript o implies evaluation at the location of the particle center. The boundary conditions for the reflected fields from the wall are

$$\mathbf{v}^{(i)} = -\mathbf{v}^{(i-1)} + \frac{\varepsilon\zeta_{\mathrm{w}}}{4\pi\mu}(\mathbf{I} - \mathbf{nn}) \cdot \nabla[\phi^{(i-1)} + \phi^{(i)}] \tag{51}$$

2.5. Flow field reflections

2.5.1. First reflection $\mathbf{v}^{(1)}$

Without the presence of the sphere no flow is generated and exists. Thus over the whole solution domain;

$$\mathbf{v}^{(1)} = 0. \tag{52}$$

Applying (50), we have:

$$\begin{aligned}\mathbf{U}^{(1)} &= -\frac{\varepsilon\zeta_{\mathrm{p}}}{4\pi\mu}[\nabla\phi^{(1)}]_{\mathrm{o}} \\ &= U_{\mathrm{p}}\mathbf{i}_z,\end{aligned} \tag{53}$$

where

$$U_{\mathrm{p}} = \frac{\varepsilon\zeta_{\mathrm{p}}E_\infty}{4\pi\mu},$$

since $\phi^{(1)}$ is known from (12).

2.5.2. Second reflection $\mathbf{v}^{(2)}$

Besides (44) and (45) the following boundary conditions should be satisfied

$$\begin{aligned}\mathbf{v}^{(2)} &= -\mathbf{v}^{(1)} + \mathbf{U}^{(1)} + \tfrac{\varepsilon\zeta_{\mathrm{p}}}{4\pi\mu}\nabla[\phi^{(1)} + \phi^{(2)}] \\ &= U_{\mathrm{p}}(\cos\theta\mathbf{i}_{\mathrm{r}} + \tfrac{1}{2}\sin\theta\mathbf{i}_\theta)\end{aligned} \quad @\ r = a, \tag{54}$$

$$\mathbf{v}^{(2)} = 0\ @\ r\to\infty. \tag{55}$$

Due to axisymmetry, the present problem can be treated by means of a stream function ψ, which is defined in spherical coordinates (r,θ) as

$$v_r = -\frac{1}{r^2 \sin\theta}\frac{\partial \psi}{\partial \theta} \qquad v_\theta = \frac{1}{r \sin\theta}\frac{\partial \psi}{\partial r}.$$

The differential equation satisfied by the stream function is

$$E^4(\psi) = 0, \tag{56}$$

where

$$E^2 = \frac{\partial^2}{\partial r^2} + \frac{1-\eta^2}{r^2}\frac{\partial^2}{\partial \eta^2}$$
$$\eta = \cos\theta$$

The boundary conditions (54) and (55) are transformed into

$$\left.\begin{aligned} \frac{\partial \psi}{\partial \eta} &= a^2 U_{\mathrm{p}} \eta \\ \frac{\partial \psi}{\partial r} &= \frac{1}{2} a U_{\mathrm{p}} (1-\eta^2) \end{aligned}\right\} @\ r = a, \tag{57}$$

$$\frac{\psi}{r^2} \to 0\ @\ r \to \infty. \tag{58}$$

The general solution for (56) is (Happel and Brenner, 1983),

$$\psi(r,\theta) = \sum_{n=2}^{\infty} (a_n r^n + b_n r^{-n+1} + c_n r^{n+2} + d_n r^{-n+3}) C_n^{-1/2}(\eta), \tag{59}$$

where $C_{\mathrm{n}}^{-1/2}$ is the Gegenbauer polynomial of order n and rank $(-1/2)$. It is related to the Lengendre polynomials as follows

$$C_n^{-1/2}(\eta) = \frac{P_{n-2}(\eta) - P_n(\eta)}{2n-1}.$$

Applying boundary conditions (57) and (58) we get:

$$a_n = 0 \quad c_n = 0 \quad d_n = 0$$
$$b_n = \begin{cases} -a^3 U_{\mathrm{p}} & n = 2 \\ 0 & n \neq 2 \end{cases}.$$

Therefore,

$$\psi^{(2)} = -\frac{1}{2} U_{\mathrm{p}} a^3 \frac{\sin^2\theta}{r}, \tag{60}$$

$$\mathbf{v}^{(2)} = U_{\mathrm{p}}\left(\frac{a}{r}\right)^3(\cos\theta\mathbf{i}_r + \frac{1}{2}\sin\theta\mathbf{i}_\theta), \tag{61}$$

represents an exact solution of the second reflection.

2.5.3. Third reflection $\mathbf{v}^{(3)}$

The boundary conditions that govern the third reflection are given by:

$$\begin{aligned}\mathbf{v}^{(3)} &= -\mathbf{v}^{(2)} + \frac{\varepsilon\zeta_{\mathrm{w}}}{4\pi\mu}(\mathbf{I}-\mathbf{nn})\cdot\nabla[\phi^{(2)}+\phi^{(3)}]\\ &= \left[\frac{3}{2}(U_{\mathrm{p}}-U_{\mathrm{w}})\frac{a^3\rho b}{(\rho^2+b^2)^{5/2}} + \frac{U_{\mathrm{w}}a^3}{2}\int_0^\infty \frac{\cosh(\xi t)-\kappa\sinh(\xi t)}{\cosh(\xi t)+\kappa\sinh(\xi t)}\mathrm{e}^{-b\xi}\xi^2 J_1(\rho\xi)\mathrm{d}\xi\right]\mathbf{i}_\rho\\ &\quad + \frac{1}{2}\frac{U_{\mathrm{p}}a^3(\rho^2-2b^2)}{(\rho^2+b^2)^{5/2}}\mathbf{i}_z \;@\; z=-b,\end{aligned} \tag{62}$$

$$\mathbf{v}^{(3)} = 0 \;@\; z\to\infty, \tag{63}$$

where

$$U_{\mathrm{w}} = \frac{\varepsilon\zeta_{\mathrm{w}}E_\infty}{4\pi\mu}$$

In terms of the stream function, the velocity components in cylindrical coordinates (ρ, z) can be expressed as

$$v_\rho = \frac{1}{\rho}\frac{\partial\psi}{\partial z} \quad v_z = -\frac{1}{\rho}\frac{\partial\psi}{\partial\rho},$$

where the stream function satisfies the differential equations

$$E^4(\psi) = 0, \tag{64}$$

and the differential operator E^2 is defined as:

$$E^2 = \frac{\partial^2}{\partial z^2} + \rho\frac{\partial}{\partial\rho}\left(\frac{1}{\rho}\frac{\partial}{\partial\rho}\right).$$

The boundary conditions (62) and (63) are transformed into:

$$\frac{\partial\psi}{\partial z} = \rho\left[\frac{3}{2}\frac{a^3\rho b}{(\rho^2+b^2)^{5/2}}(U_{\mathrm{p}}-U_{\mathrm{w}}) + \frac{U_{\mathrm{w}}a^3}{2}\int_0^\infty \frac{\cosh(\xi t)-\kappa\sinh(\xi t)}{\cosh(\xi t)+\kappa\sinh(\xi t)}\mathrm{e}^{-b\xi}\xi^2 J_1(\rho\xi)\mathrm{d}\xi\right], \tag{65}$$

$$\frac{\partial\psi}{\partial\rho} = -\frac{\rho}{2}\frac{U_{\mathrm{p}}a^3(\rho^2-2b^2)}{(\rho^2+b^2)^{5/2}}, \tag{66}$$

at $z = -b$ and

$$\psi = 0 \tag{67}$$

at $z \to \infty$.

Equation (64) can be separated into two differential equations (Sonshine et al., 1966):

$$E^2(W) = 0, \tag{68}$$

$$E^2(\psi) = W. \tag{69}$$

Multiplying both sides of (68) by $\rho J_1(\rho\xi)$ and integrating with respect to ρ over the $(0,\infty)$ domain yields:

$$\frac{d^2\Omega}{dz^2} - \xi^2\Omega = 0, \tag{70}$$

where Ω is the Hankel transform

$$\Omega(\xi, z) = \int_0^\infty w(\rho, z)\rho J_1(\rho\xi)d\rho.$$

The inverse transform is given by

$$w(\rho, z) = \int_0^\infty \Omega(\xi, z)\xi J_1(\rho\xi)\, d\xi,$$

where

$$w(\rho, z) = \frac{W(\rho, z)}{\rho}.$$

The general solution of (70) is:

$$\Omega(\xi, z) = A(\xi)e^{-\xi(z+b)} + B(\xi)e^{\xi(z+b)}, \tag{71}$$

where $A(\xi)$ and $B(\xi)$ are yet unknown functions of the dummy variable ξ. Now we apply the following Hankel transform:

$$Q(\xi, z) = \int_0^\infty q(\rho, z)\rho J_1(\rho\xi)\, d\rho,$$

where

$$q(\rho, z) = \frac{\psi(\rho, z)}{\rho},$$

to (69) and obtain:

$$\frac{d^2Q}{dz^2} - \xi^2 Q = A(\xi)e^{-\xi(z+b)} + B(\xi)e^{\xi(z+b)}. \tag{72}$$

The general solution of (72) with boundary condition (67) is:

$$Q = C(\xi)\mathrm{e}^{-\xi(z+b)} + D(\xi)(z+b)\mathrm{e}^{-\xi(z+b)}. \tag{73}$$

Consequently, with the aid of the inverse Hankel transform,

$$q(\rho, z) = \int_0^\infty Q(\xi, z)\xi J_1(\rho\xi)\,\mathrm{d}\xi,$$

we obtain:

$$\psi(\rho, z) = \rho\int_0^\infty [C(\xi)\mathrm{e}^{-\xi(z+b)} + D(\xi)(z+b)\mathrm{e}^{-\xi(z+b)}]\xi J_1(\rho\xi)\,\mathrm{d}\xi. \tag{74}$$

Applying (65) and (66) to (74), respectively, we obtain

$$\int_0^\infty [\xi C(\xi) - D(\xi)]\xi J_1(\rho\xi)\,\mathrm{d}\xi = -\frac{3}{2}\frac{a^3\rho b}{(\rho^2+b^2)^{5/2}}(U_\mathrm{p} - U_\mathrm{w}) - \frac{U_\mathrm{w}a^3}{2}\int_0^\infty \frac{\cosh(\xi t) - \kappa\sinh(\xi t)}{\cosh(\xi t) + \kappa\sinh(\xi t)}\mathrm{e}^{-b\xi}\xi^2 J_1(\rho\xi)\,\mathrm{d}\xi, \tag{75}$$

and

$$\int_0^\infty C(\xi)\xi^2 J_0(\rho\xi)\,\mathrm{d}\xi = \frac{1}{2}\frac{U_\mathrm{p}a^3(2b^2-\rho^2)}{(\rho^2+b^2)^{5/2}}. \tag{76}$$

Since

$$\int_0^\infty \mathrm{e}^{-b\xi}\xi^2 J_1(\rho\xi)\,\mathrm{d}\xi = \frac{3\rho b}{(\rho^2+b^2)^{5/2}},$$

and

$$\int_0^\infty \mathrm{e}^{-b\xi}\xi^2 J_0(\rho\xi)\,\mathrm{d}\xi = \frac{2b^2-\rho^2}{(\rho^2+b^2)^{5/2}}.$$

(Gradshteyn and Ryzhik, 1994), we recover from (75) and (76),

$$\xi C(\xi) - D(\xi) = \frac{a^3\mathrm{e}^{-b\xi}\xi}{2}\left[\frac{2\kappa\sinh(\xi t)}{\cosh(\xi t) + \kappa\sinh(\xi t)}U_\mathrm{w} - U_\mathrm{p}\right],$$

and

$$C(\xi) = \frac{U_\mathrm{p}a^3}{2}\mathrm{e}^{-b\xi}.$$

Thus, it is obtained that

$$D(\xi) = \frac{a^3\mathrm{e}^{-b\xi}\xi}{2}\left[2U_\mathrm{p} - \frac{2\kappa\sinh(\xi t)}{\cosh(\xi t) + \kappa\sin h(\xi t)}U_\mathrm{w}\right],$$

and

$$\psi(\rho,z)=\frac{a^3\rho}{2}\int_0^\infty\{U_{\rm p}+\left[2U_{\rm p}-\frac{2\kappa\sinh(\xi t)}{\cosh(\xi t)+\kappa\sinh(\xi t)}U_{\rm w}\right](z+b)\xi\}{\rm e}^{-(z+2b)\xi}\xi J_1(\rho\xi)\,{\rm d}\xi.$$

Therefore,

$$\begin{aligned}\mathbf{v}^{(3)}=&\left(\frac{a^3}{2}\int_0^\infty\left\{\left[U_{\rm p}-\frac{2\kappa\sinh(\xi t)}{\cosh(\xi t)+\kappa\sinh(\xi t)}U_{\rm w}\right]\right.\right.\\&+\left.\left[\frac{2\kappa\sinh(\xi t)}{\cosh h(\xi t)+\kappa\sinh(\xi t)}U_{\rm w}-2U_{\rm p}\right](z+b)\xi\right\}{\rm e}^{-(z+2b)\xi}\xi^2J_1(\rho\xi)\,{\rm d}\xi\Big)\mathbf{i}_\rho\\&+\left(-\frac{a^3}{2}\int_0^\infty\{U_{\rm p}+\left[2U_{\rm p}-\frac{2\kappa\sinh(\xi t)}{\cosh(\xi t)+\kappa\sinh(\xi t)}U_{\rm w}\right](z+b)\xi\}{\rm e}^{-(z+2b)\xi}\xi^2J_0(\rho\xi)\,{\rm d}\xi\right)\mathbf{i}_z,\end{aligned}$$

is an exact solution of the third reflection. According to (50), we have:

$$\mathbf{U}^{(2)}=-\frac{\varepsilon\xi_{\rm p}}{4\pi\mu}[\nabla\phi^{(3)}]_{\rm o}+[\mathbf{v}^{(3)}]_{\rm o}+\frac{1}{6}a^2[\nabla^2\mathbf{v}^{(3)}]_{\rm o}=\left[\lambda^3\left(-\frac{5}{8}+\frac{I_1}{2}+\frac{\gamma I_2}{2}\right)+\lambda^5\left(\frac{1}{4}-\frac{\gamma I_3}{6}\right)\right]U_{\rm p}\mathbf{i}_z,\tag{79}$$

where

$$I_3=\int_0^\infty\frac{2\kappa\sinh(\xi\beta)}{\cosh(\xi\beta)+\kappa\sinh(\xi\beta)}\xi^4{\rm e}^{-2\xi}\,{\rm d}\xi.$$

2.5.4. Fourth reflection $\mathbf{v}^{(4)}$

The fourth reflection $\mathbf{v}^{(4)}$ can approximately be obtained by (Keh and Anderson, 1985)

$$\mathbf{v}^{(4)}(\mathbf{r})=\frac{\varepsilon\zeta_{\rm p}}{4\pi\mu}\left\{-\frac{1}{2}\left(\frac{a}{r}\right)^3\left[3\frac{\mathbf{rr}}{r^2}-\mathbf{I}\right]\cdot[\nabla\phi^{(3)}]_{\rm o}+\left[\frac{5}{2}\frac{a^3}{r^5}\mathbf{rrr}+\frac{5}{6}\left(\frac{a}{r}\right)^5\left(2\mathbf{Ir}-5\frac{\mathbf{rrr}}{r^2}\right)\right]:[\nabla\nabla\phi^{(3)}]_{\rm o}+\cdots\right\}.\tag{80}$$

Substitution of (31) into the above equations yields:

$$\begin{aligned}\mathbf{v}^{(4)}=&U_{\rm p}\left[-\frac{1}{2}\left(\frac{a}{r}\right)^3\lambda^3\left(\frac{1}{4}-I_1\right)\left(\cos\theta\mathbf{i}_r+\frac{1}{2}\sin\theta\mathbf{i}_\theta\right)\right.\\&\left.+\frac{5}{4}\left(\frac{a}{r}\right)^2\lambda^4\left(\frac{3}{8}-I_2\right)\left(\frac{1}{2}\sin^2\theta-\cos^2\theta\right)\mathbf{i}_r\right]+{\rm o}(\lambda^4a^4,\lambda^5a^3).\end{aligned}\tag{81}$$

2.5.5. Fifth reflection $\mathbf{v}^{(5)}$

The boundary conditions governing the fifth velocity reflection are:

$$\mathbf{v}^{(5)} = -\mathbf{v}^{(4)} + \frac{\varepsilon\zeta_{\mathrm{w}}}{4\pi\mu}(\mathbf{I}-\mathbf{nn})\cdot\nabla[\phi^{(4)}+\phi^{(5)}] \;@\; z=-b, \tag{82}$$

$$\mathbf{v}^{(5)}\to 0 \;@\; z\to\infty, \tag{83}$$

where $\phi^{(4)}$ and $\phi^{(5)}$ are given by (36) and (42), respectively. Similar to the procedure that was applied to obtain the third reflection, we use the Hankel transform twice to derive $\mathbf{v}^{(5)}$. Consequently, we get:

$$\begin{aligned}\mathbf{U}^{(3)} &= -\frac{\varepsilon\zeta_{\mathrm{p}}}{4\pi\mu}[\nabla\phi^{(5)}]_{\mathrm{o}} + [\mathbf{v}^{(5)}]_{\mathrm{o}} + \frac{1}{6}a^2[\nabla^2\mathbf{v}^{(5)}]_{\mathrm{o}} \\ &= \left\{\lambda^6\left[-\frac{25}{256}+\frac{5}{32}(3I_2-I_1)+\frac{1}{16}(2-\gamma)I_1(4I_1-1)\right]+\mathrm{o}(\lambda^8)\right\}U_{\mathrm{p}}\mathbf{i}_z.\end{aligned} \tag{84}$$

2.5.6. The approximate flow field and electrophoretic velocity

The sum of the foregoing velocity reflections:

$$\mathbf{v} = \mathbf{v}^{(1)}+\mathbf{v}^{(2)}+\mathbf{v}^{(3)}+\mathbf{v}^{(4)}+\mathbf{v}^{(5)}+\cdots, \tag{85}$$

and electrophoretic reflection velocities of the particle

$$\begin{aligned}\mathbf{U} =& \mathbf{U}^{(1)}+\mathbf{U}^{(2)}+\mathbf{U}^{(3)}+\cdots \\ =& \left\{1-\frac{5}{8}\lambda^3\left[1-\frac{4}{5}(I_1+\gamma I_2)\right]+\frac{1}{4}\lambda^5\left(1-\frac{2}{3}\gamma I_3\right)\right. \\ & \left.-\frac{25}{256}\lambda^6\left[1-\frac{8}{5}(3I_2-I_1)-\frac{16}{25}(2-\gamma)I_1(4I_1-1)\right]+\mathrm{o}(\lambda^8)\right\}U_{\mathrm{p}}\mathbf{i}_z\end{aligned} \tag{86}$$

represent approximate solutions for the flow field generated by the electric field and particle electrophoretic velocity.

3. Results and discussion

The electrophoretic velocity (86) depends on four dimensionless parameters β, λ, κ and γ. The first two determine the system's geometrical configuration and the last two depend on the system's electrical phenomenological coefficients.

Fig. 2 shows plots of the electric field around the particle and inside the dielectric layer. It vividly shows that a tangential component of the electric field near the dielectric wall does not vanish and is largest at about one particle radius from the symmetry axis of the system. In case the applied electric field points toward the dielectric wall its tangential component near the wall

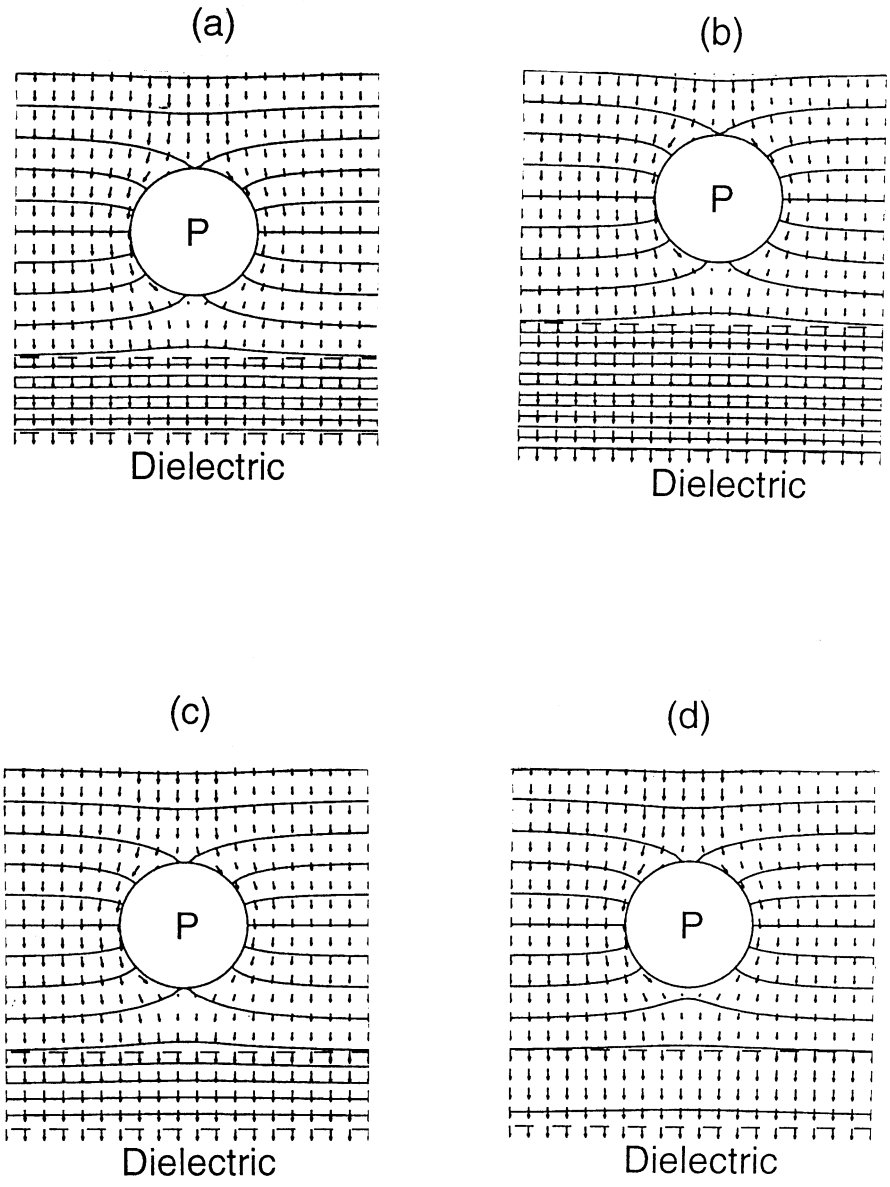

Fig. 2. Electric potential distribution around a charged particle for $\lambda = 0.5$. (a) $\kappa = 3$, $\beta = 0.6$; (b) $\kappa = 3$, $\beta = 1$; (c) $\kappa = 2$, $\beta = 0.6$; and (d) $\kappa = 0.5$, $\beta = 0.6$.

points toward the axis of symmetry. The opposite is true for E_∞ pointing away from the dielectric wall. It is also demonstrated that the electric field arrows are squeezed between the particle and the dielectric wall, the higher the values of β and κ the more they are tilted with respect to the E_∞ direction. As explained later, the foregoing observations make it easy to understand the electric wall effect mechanism.

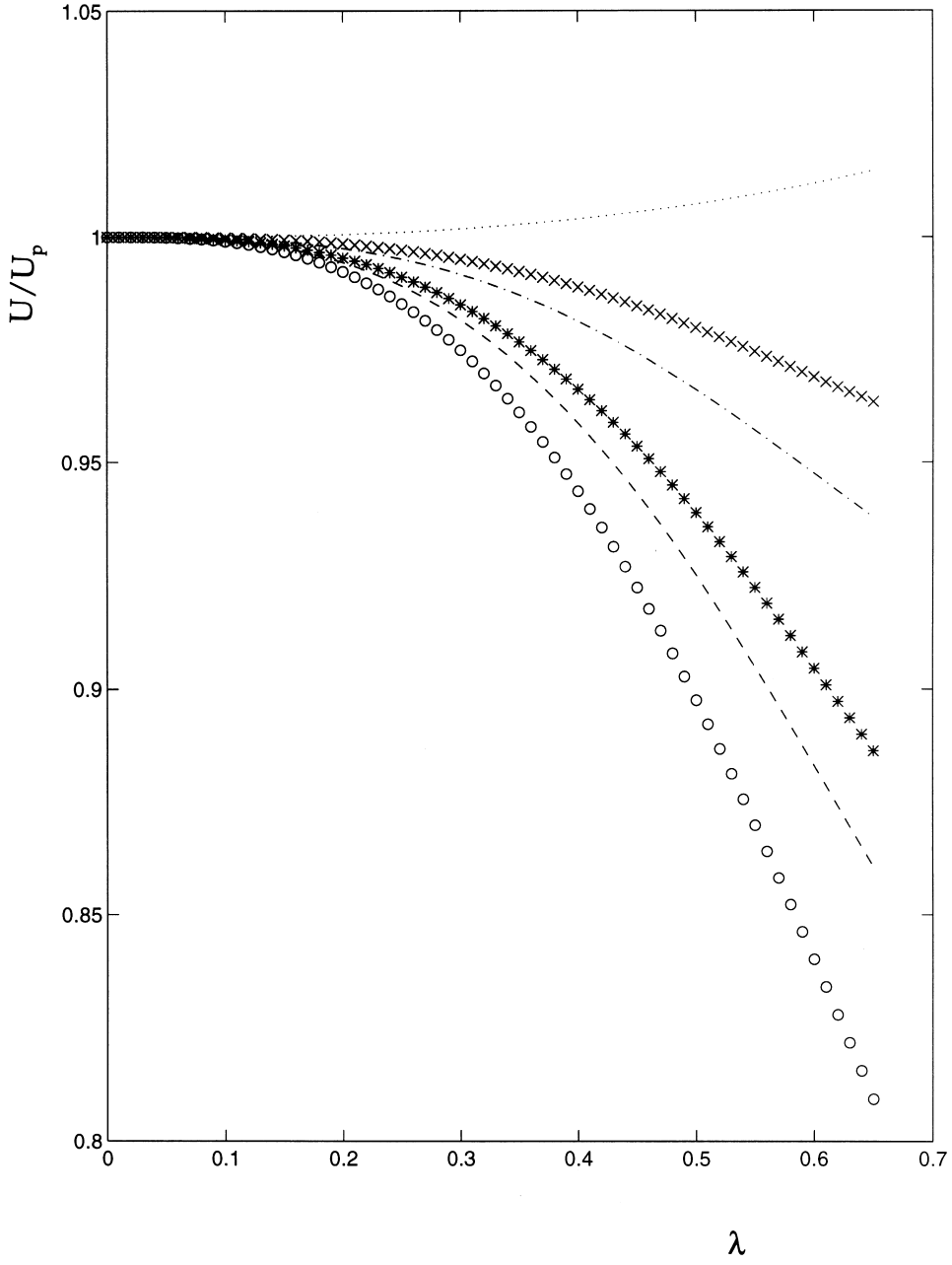

Fig. 3. Effect of zeta-potential ratio (γ) on the particle electrophoretic motion for $\beta = 0.8$ and $\kappa = 3$. (o) $\gamma = 2$; (- -) $\gamma = -1$; (*) $\gamma = -0.5$; (- ·) $\gamma = 0.5$; (x) $\gamma = 1$; (. . .) $\gamma = 2$.

Fig. 3 depicts the electrophoretic velocity dependence on λ for various values of γ both positive and negative and for constant values of $\beta = 0.8$ and $\kappa = 3$. Clearly, the closer the particle is to the wall (higher values of λ) the higher is the velocity retardation or gain, where

the former occurs for negative γ values and the latter for high positive γ values. In the discussion that follows we try to explore how these different parameters affect the various mechanisms that govern particle motion.

Two competing phenomenon affect particle velocity retardation or gain, the hydrodynamic, and the electric wall effects. The purely hydrodynamic wall effect (solved by Keh and Anderson, 1985) always causes velocity retardation regardless of particle direction of motion, a fact also known from low Reynolds hydrodynamic theory (Happel and Brenner, 1983). Notwithstanding, the electrical wall effect may cause either velocity retardation or gain depending on the sign of γ. Let us discuss this statement.

Smoluchowski's solution states that the direction of a charged particle electrophoretic migration is determined by the sign of its zeta potential ζ_p and the direction of the applied electric field E_∞. To simplify the discussion we, henceforth, assume that E_∞ points toward the dielectric wall. Thus, a positively charged particle tends to move toward the dielectric wall and a negatively charged particle tends to migrate away from it. The direction of the electroosmotic flow *near* the dielectric wall is governed by the direction of the tangential component of the *applied* electrical field near the wall and the sign of ζ_w. In case E_∞ points toward the dielectric wall, the tangential component points toward the system's axis of symmetry (see Fig. 2). Hence, for positive ζ_w the fluid near the wall is induced to move radially away from the symmetry axis of the system. That, in turn, induces an axial downward flow along the symmetry axis so that mass conservation requirements are satisfied. The axial flow induces a drag force on the sphere that points toward the dielectric plane. Obviously, the opposite is true for negative wall zeta potentials ζ_w. Consequently, for a particle that tends to move toward the dielectric wall ($\zeta_p > 0$) the electroosmotic flow tends to increase its velocity in case $\zeta_w > 0$, and retard it for $\zeta_w < 0$. Clearly, the opposite is true for a particle moving away from the wall for which $\zeta_p < 0$. Now, for positive ζ_p and ζ_w, if we reverse the direction of E_∞, the particle moves away from the dielectric plane but the electroosmotic flow is also reversed causing a velocity increase. Similarly, negative values of ζ_p and ζ_w cause a velocity increase only this time the particle moves toward the plane. Thus, the following statement can summarize simply the foregoing discussion on the electric wall effect: positive zeta potential ratios γ result in an enhanced particle velocity while negative γ ratios cause velocity retardation. Evidently, the higher the value of $\gamma = \zeta_w/\zeta_p$ the stronger is the induced electroosmotic flow and the more pronounced is the electric effect. It must be stressed that this enhancement/retardation mechanism stems solely from incorporating the dielectric layer into the solution model. It is totally absent in previously dealt problems in which the bounding wall was a perfect conductor.

Finally, in case $\gamma < 0$ the electric and hydrodynamic wall effects combine and the presence of the wall causes the particle to slow down (when compared with its Smoluchowski's velocity). For $\gamma > 0$ the electric and hydrodynamic wall effects oppose each other, and as γ increases, they almost cancel each other. Eventually, for γ values larger than 2, the electric force overcomes the hydrodynamic retardation effect and the particle moves faster than its Smoluchowski's velocity.

The effects of $\beta = t/b$ and $\kappa = \varepsilon/\varepsilon_w$ on the electrophoretic velocity are illustrated in Fig. 4(a)–(d). It is vividly seen from Fig. 4(a) and (c) that thinner dielectric layers (β decreasing) and higher dielectric constants (κ decreasing) result in a weaker electric wall effect. That is due to a

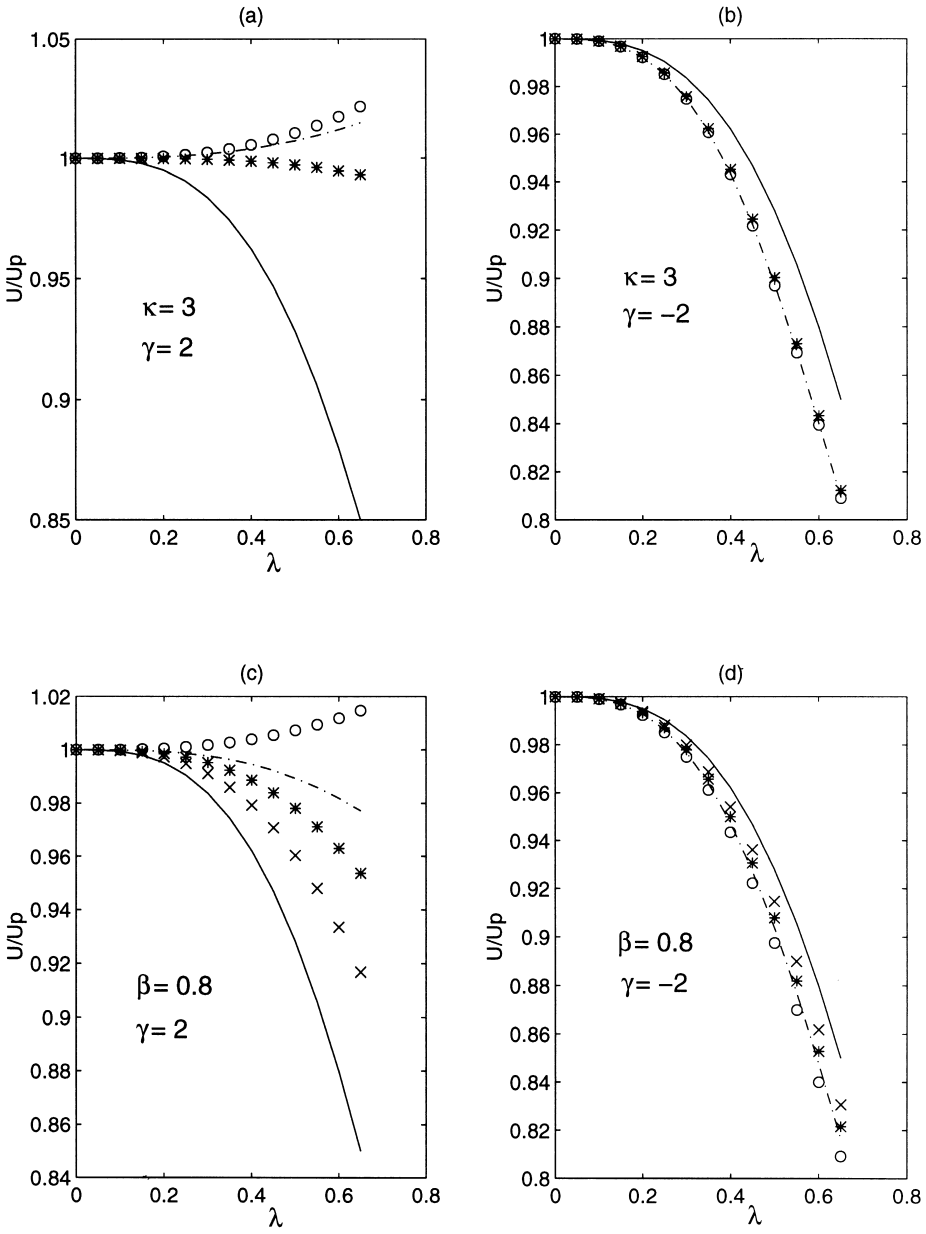

Fig. 4. Effects of the dielectric thickness (β) and the dielectric constant (κ) on the particle electrophoretic motion. In (a) and (b): (o) $\beta = 1.2$; (- ·) $\beta = 0.8$; (*) $\beta = 0.4$; (-) $\beta = 0$ (Keh and Anderson, 1985). In (c) and (d): (o) $\kappa = 3$; (- ·) $\kappa = 1.5$; (*) $\kappa = 1$; (x) $\kappa = 0.5$; (-) $\kappa = 0$ (Keh and Anderson, 1985).

corresponding decrease in the tangential component of the electric field near the dielectric wall. Consequently, the induced electroosmotic flow is slower and the resulting drag force applied on the sphere is decreased. For the limiting cases of $\beta = 0$ or $\kappa = 0$, the results coincide with those given by Keh and Anderson (1985).

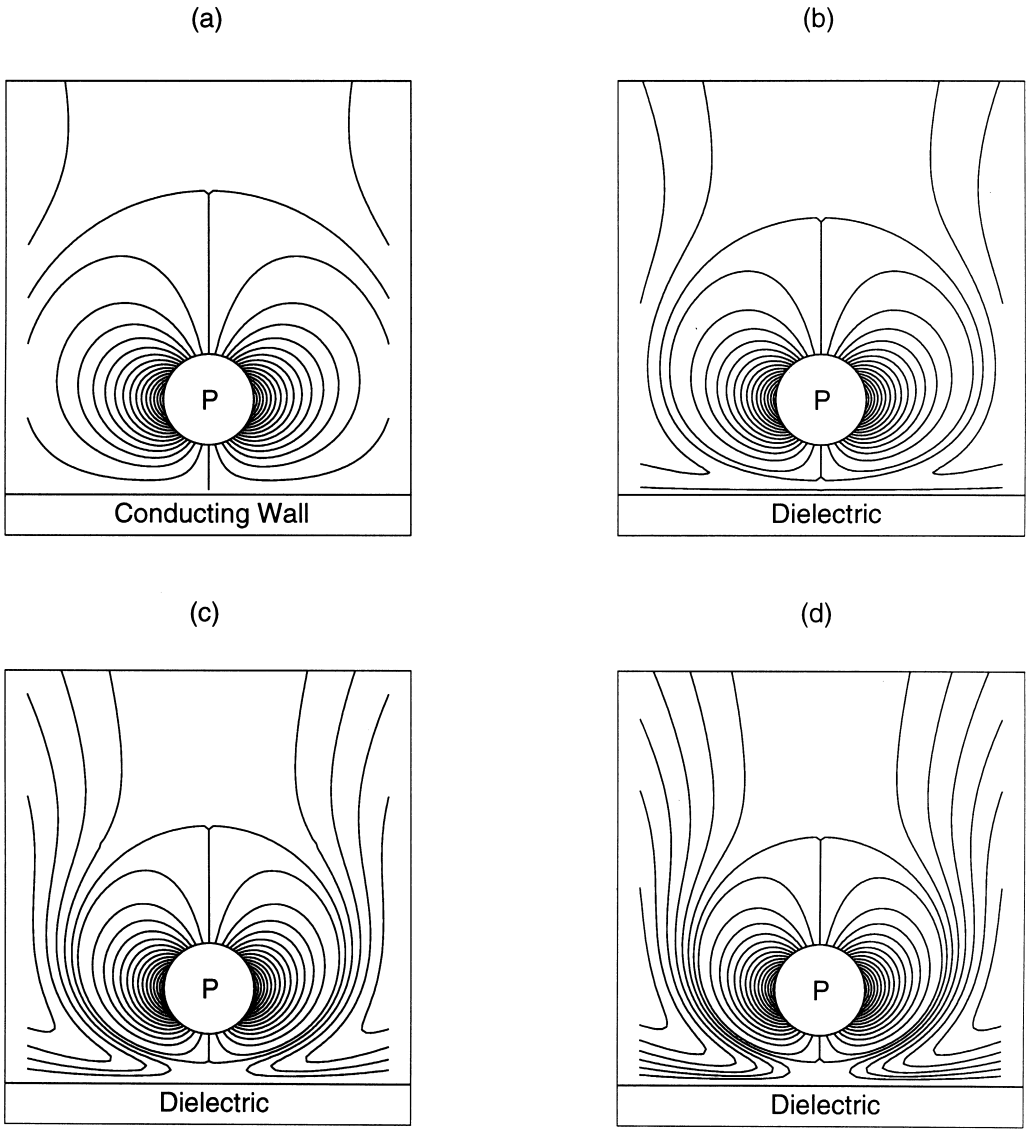

Fig. 5. Velocity field induced by a particle moving towards the dielectric wall that possesses a negative zeta-potential. The particle moves slower than its Smoluchowski's velocity. Given $\lambda = 0.5$, $\beta = 0.8$, $\gamma = -2$. (a) $\kappa = 0$ (Keh and Anderson, 1985); (b) $\kappa = 0.5$; (c) $\kappa = 1.5$; (d) $\kappa = 3$.

Streamline maps of the flow field induced by a particle for negative and positive values of γ are presented in Figs. 5 and 6, respectively, and in turn compared with that obtained by Keh and Anderson (1985). The latter map possesses a single stagnation point that exists in the field bulk away from the particle and the wall. Notwithstanding, an additional stagnation point is formed in case β and κ do not vanish, the second point located between the sphere and the

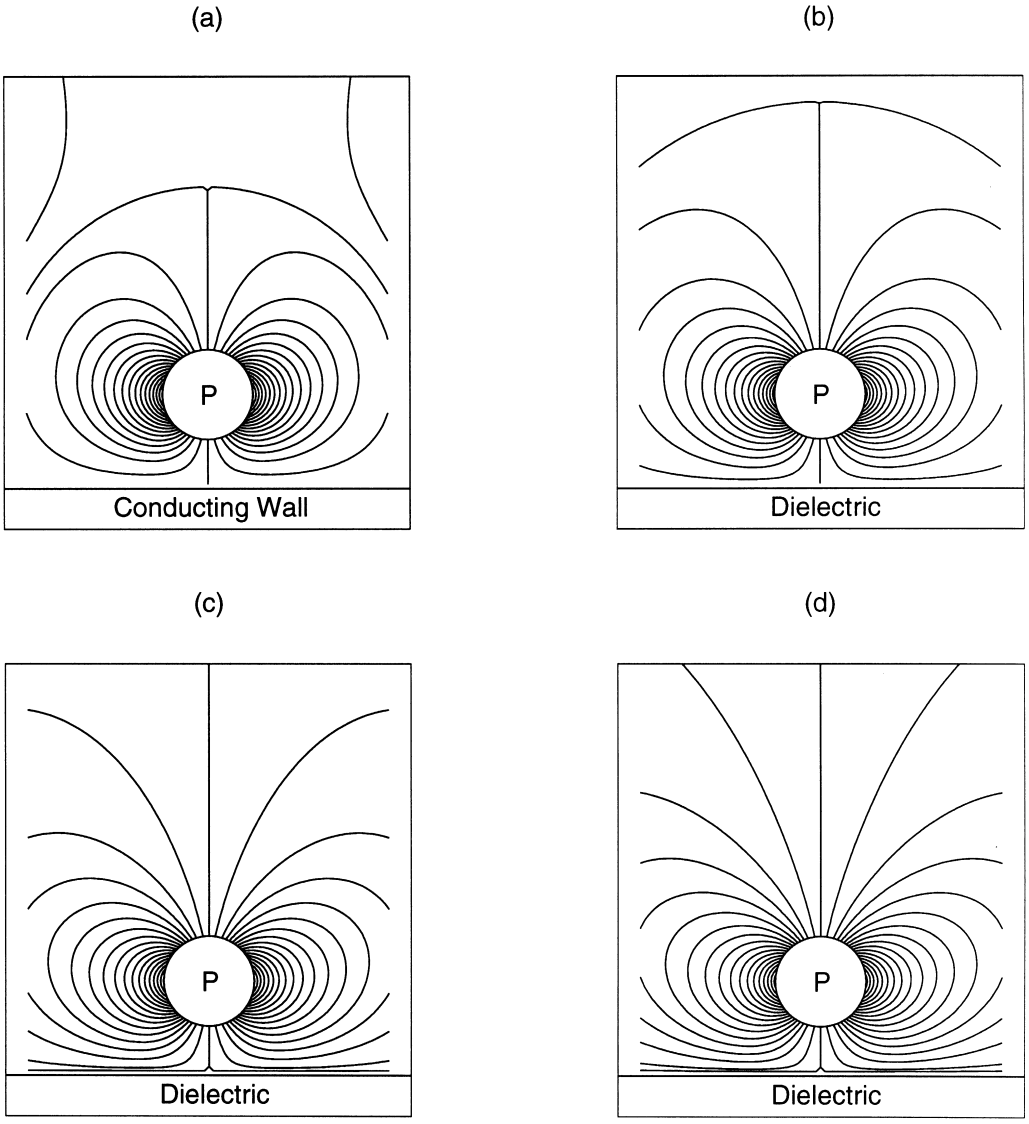

Fig. 6. Velocity field induced by a particle moving towards the dielectric wall that possesses a positive zeta-potential. The particle moves faster than its Smoluchowski's velocity. Given $\lambda = 0.5$, $\beta = 0.8$, $\gamma = 2$. (a) $\kappa = 0$ (Keh and Anderson, 1985); (b) $\kappa = 0.5$; (c) $\kappa = 1.5$; (d) $\kappa = 3$.

plane. For $\gamma = 2$ the stagnation point is located closer to the plane than that obtained for $\gamma = -2$, and the map of the latter case is almost similar to that of Keh and Anderson (1985). That observation supports qualitatively the previous discussion about the opposing hydrodynamic and electrical wall effects in case γ is positive.

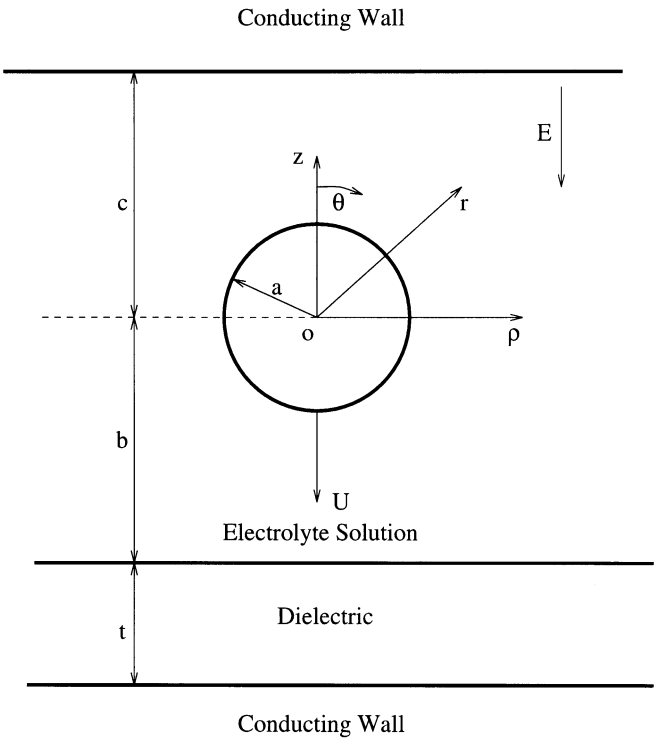

Fig. 7. The electrophoretic system configuration of a particle positioned between two parallel planar walls.

4. Solution for the perpendicular electrophoretic motion of a particle between a conducting plane and a dielectric planar wall

In this section the electrophoretic motion of a spherical particle perpendicular to two parallel planar walls, one perfectly conducting and the other a dielectric, is studied (Fig. 7). The distance from the particle center to the conducting wall is c.

The boundary conditions in this case are,

$$\mathbf{n} \cdot \nabla\phi = 0 \ @ \ r = a, \tag{87}$$

$$\phi_w = 0; @ \ z = -(b + t), \tag{88}$$

$$\left.\begin{array}{c} \phi = \phi_w \\ \kappa(\mathbf{n} \cdot \nabla\phi) = \mathbf{n} \cdot \nabla\phi_w \end{array}\right\} @ \ z = -b, \tag{89}$$

$$\phi = \phi_0 \text{ (constant)} @ \ z = c, \tag{90}$$

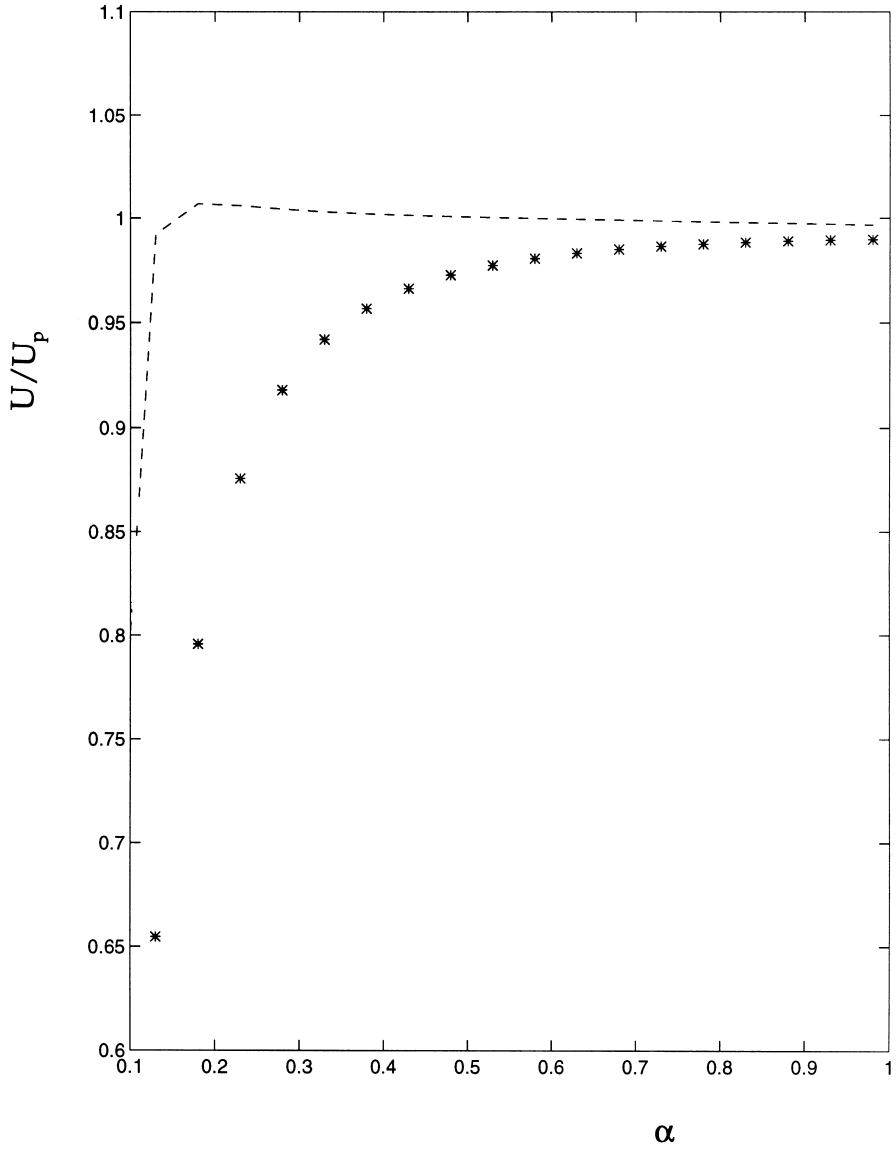

Fig. 8. The electrophoretic velocity of a particle translating perpendicular to two parallel planar walls vs α for constant $a/(b + c) = 0.1$. (- -) $\gamma = 2$; (*) $\gamma = -2$.

for the electric field,

$$\mathbf{v} = \mathbf{U} + \frac{\varepsilon\zeta_p}{4\pi\mu}\nabla\phi \ @ \ r = a, \tag{91}$$

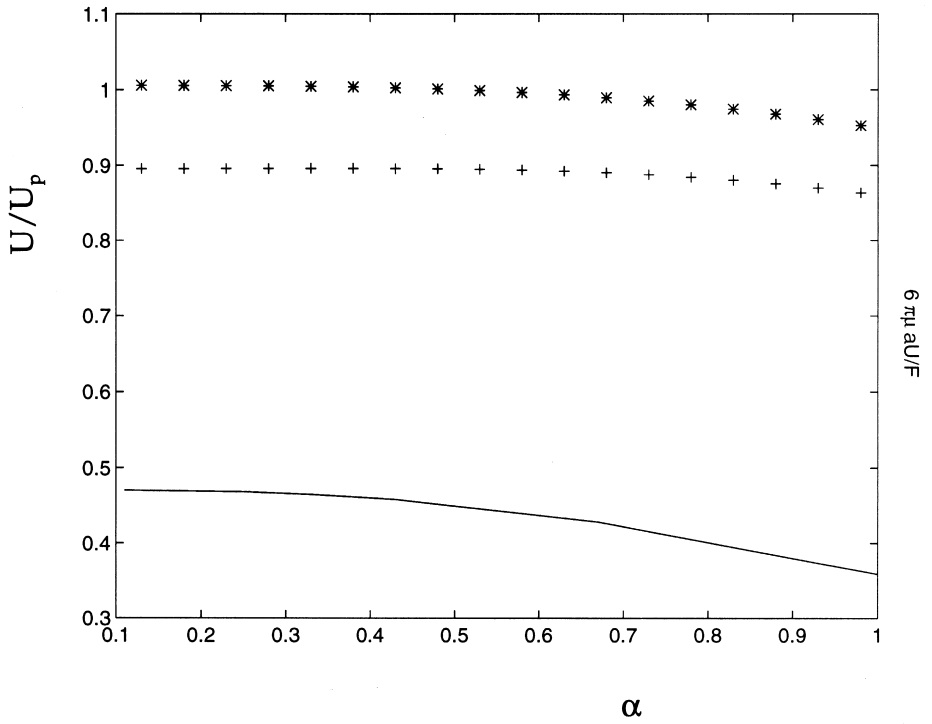

Fig. 9. The electrophoretic velocity and the Stokes mobility $6\pi\mu aU/F$ (Ganatos et al., 1980) vs α for constant $\lambda_1 = 0.5$. (-) Ganatos et al., 1980; (*) $\gamma = 2$; (+) $\gamma = -2$.

$$\mathbf{v} = \frac{\varepsilon\zeta_w}{4\pi\mu}(\mathbf{I} - \mathbf{nn}) \cdot \nabla\phi \ @ \ z = -b, \tag{92}$$

$$\mathbf{v} = 0 \ @ \ z = c, \tag{93}$$

for the flow field.

A single new non-dimensional parameter must be introduced here.

$$\lambda_2 = \frac{a}{c}.$$

For the sake of symmetry we shall redefine λ as $\lambda_1 = a/b$ and define the useful parameter $\alpha = \lambda_2/\lambda_1 = b/c$.

Following the procedure in Section 2, we solve the above problem by the method of reflections with $\lambda_1 < 1$ and $\lambda_2 < 1$. Without the presence of the particle, the electric field E is uniform

$$E = -\frac{\phi_0}{b + c + \kappa t}$$

Solution of the first four reflections yields the electrophoretic velocity of the particle

(a)

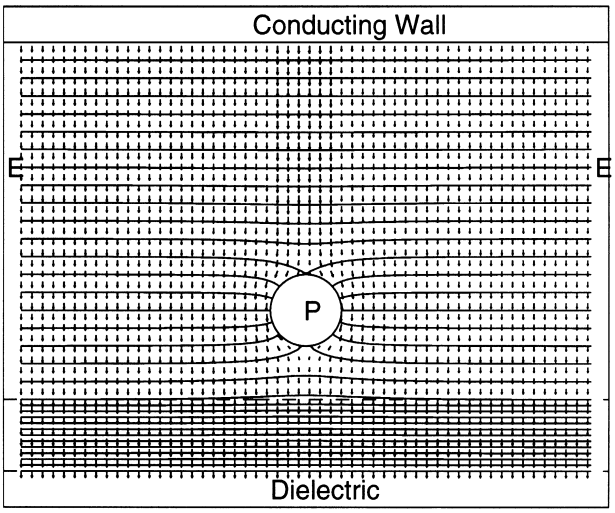

(b)

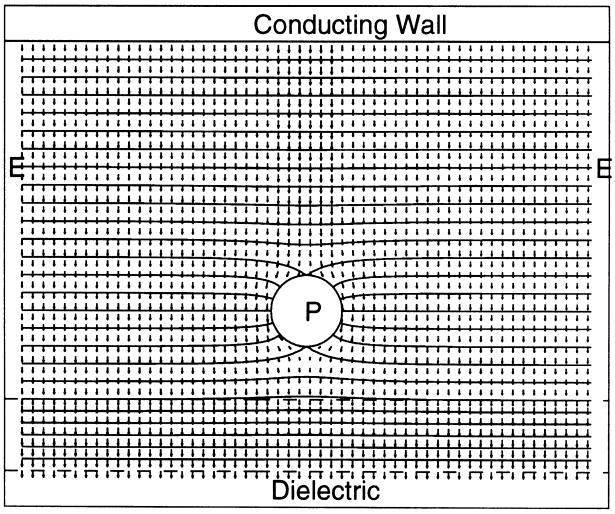

Fig. 10. The electric field around a charged particle suspended between a conducting and a dielectric wall for constant $\lambda_1 = 0.4$ and $\beta = 0.8$. (a) $\kappa = 3$; (b) $\kappa = 1.5$.

(a)

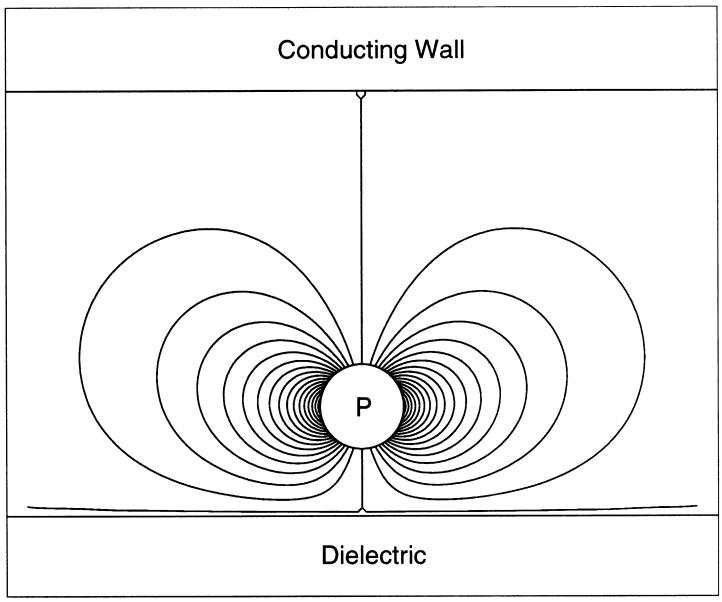

(b)

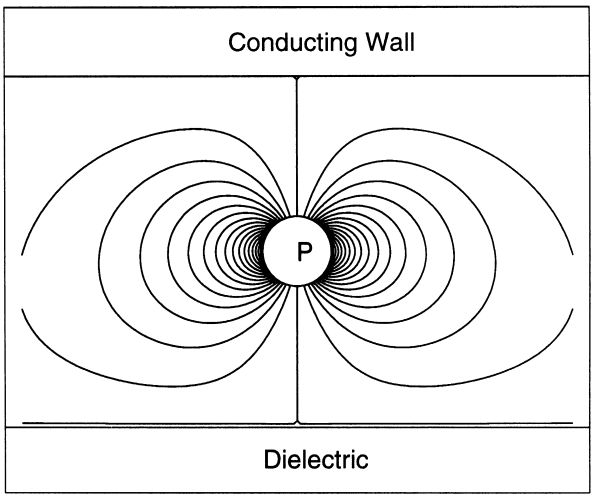

Fig. 11. The velocity field around a charged particle moving from the conducting towards the dielectric wall that possesses a positive zeta-potential, for $\gamma = 1$, $\kappa = 3$, $\beta = 0.8$ and $a/(b + c) = 0.1$. (a) $\lambda_1 = 0.4$ and $\alpha = 0.3$; (b) $\lambda_1 = 0.2$ and $\alpha = 1$.

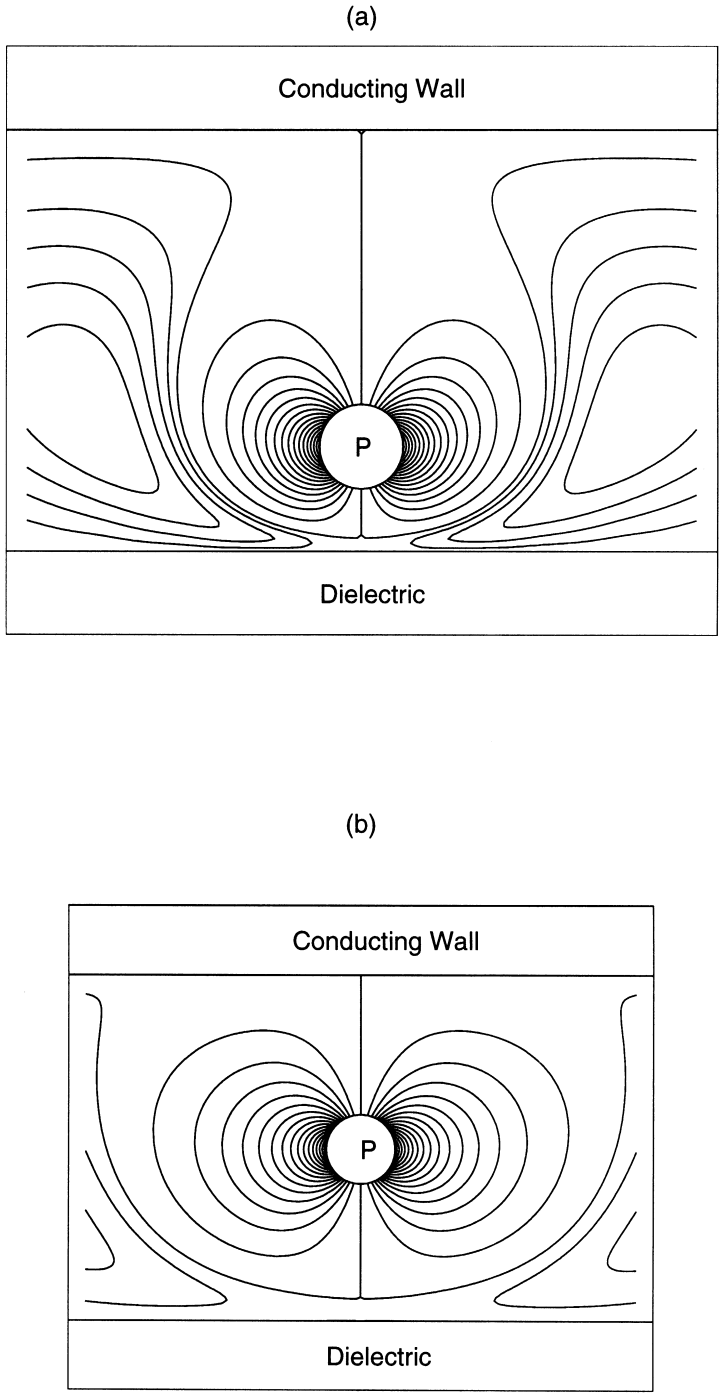

Fig. 12. The velocity field around a charged particle moving from the conducting towards the dielectric wall that possesses a negative zeta-potential, for $\gamma = -1$, $\kappa = 3$, $\beta = 0.8$ and $a/(b + c) = 0.1$. (a) $\lambda_1 = 0.4$ and $\alpha = 0.3$; (b) $\lambda_1 = 0.2$ and $\alpha = 1$.

$$\mathbf{U} = \left(\left\{ 1 - \frac{(\lambda_1+\lambda_2)^3}{2} (I_4 + \int_0^\infty [E(\xi)\mathrm{e}^{(1+\alpha)\xi} + F(\xi)\mathrm{e}^{-(1+\alpha)\xi} + G(\xi)(1+\alpha)\xi\mathrm{e}^{(1+\alpha)\xi} + H(\xi)(1+\alpha)\xi\mathrm{e}^{-(1+\alpha)\xi}]\xi^2 \,\mathrm{d}\xi + \frac{(\lambda_1+\lambda_2)^5}{6} \int_0^\infty [-G(\xi)\mathrm{e}^{(1+\alpha)\xi} + H(\xi)\mathrm{e}^{-(1+\alpha)\xi}]\xi^4 \,\mathrm{d}\xi \right\} + O[(\lambda_1+\lambda_2)^6] \right) U_\mathrm{p}\mathbf{i}_z. \tag{94}$$

Integral I_4 and Coefficients $E(\xi)$, $F(\xi)$, $G(\xi)$ and $H(\xi)$ are given in Appendix A.

Numerical results for the translational velocity of a particle undergoing electrophoresis in a direction perpendicular to two parallel planar walls are depicted in Fig. 8, which illustrates the comparatively stronger effect of γ on the electrophoretic velocity of a particle in the vicinity of the dielectric wall.

When the electroosmotic velocity induces a drag force that enhances the electrophoretic forces (γ positive) its effect is strongest for particle positions near the dielectric wall ($0 < \alpha < 0.2$). When the electroosmotic velocity induces a drag force that opposes the electrophoretic forces (γ negative) it adds to the hydrodynamic retardation effect and the particle experiences only a gradual increase in its velocity as α increases.

A comparison between the normalized electrophoretic velocity U/U_p and the non-dimensional Stokes mobility $6\pi\mu aU/F$ (Ganatos et al., 1980) is illustrated in Fig. 9. For $0 < \alpha < 0.4$ the presence of the conducting wall is insignificant. It is also shown that the electrophoretic velocity is less sensitive to wall effects than that encountered in an hydrodynamic case.

Fig. 10 displays the electric field between two parallel walls, while Figs. 11 and 12 show the flow streamlines induced by a particle leaving or approaching the dielectric wall. The pattern possesses a similar topology to that of Keh and Anderson (1985) in the region between the particle and the conducting wall and to that of Section 2 in the region between the particle and the dielectric.

Appendix A

The following integral and coefficients appear in Section 4 and are given below:

$$I_4 = \int_0^\infty [A(\xi)\mathrm{e}^{(1+\alpha)\xi} - B(\xi)\mathrm{e}^{-(1+\alpha)\xi}]\xi^2 \,\mathrm{d}\xi, \tag{A1}$$

$$E(\xi) = \{\mathrm{e}^{-(1+\alpha)\xi} \frac{(1+\alpha)^4}{\alpha^2}\xi^2 - \mathrm{e}^{-(1+\alpha)\xi}\sinh^2\left[\frac{(1+\alpha)^4}{\alpha^2}\xi^2\right] - \frac{(1+\alpha)^2}{\alpha}\xi\sinh[(1+\alpha)\xi] + \sinh\left[\frac{(1+\alpha)^2}{\alpha}\xi\right]\sinh\left[\frac{(1+\alpha)}{\alpha}\xi\right] - \frac{\gamma}{2}[\mathrm{e}^{-(1+\alpha)\xi} + A(\xi) + B(\xi)]\frac{(1+\alpha)^4}{\alpha^2}\xi^2\} \Big/ \left\{ \frac{(1+\alpha)^4}{\alpha^2}\xi^2 - \sinh^2\left[\frac{(1+\alpha)^2}{\alpha}\xi\right] \right\} \tag{A2}$$

$$F(\xi)=\left\{\frac{(1+\alpha)^2}{\alpha}\xi\sinh[(1+\alpha)\xi]-\sinh\left[\frac{(1+\alpha)^2}{\alpha}\xi\right]\sinh\left[\frac{(1+\alpha)}{\alpha}\xi\right]+\frac{\gamma}{2}[e^{-(1+\alpha)\xi}+A(\xi)+B(\xi)]\frac{(1+\alpha)^4}{\alpha^2}\xi^2\right\}/\left\{\frac{(1+\alpha)^4}{\alpha^2}\xi^2-\sinh^2\left[\frac{(1+\alpha)^2}{\alpha}\xi\right]\right\}, \tag{A3}$$

$$G(\xi)=\left(-\frac{(1+\alpha)^2}{\alpha}\xi e^{-(1+\alpha)\xi}+e^{-\frac{(1+\alpha)}{\alpha}\xi}\sinh\left[\frac{(1+\alpha)^2}{\alpha}\xi\right]+\frac{\gamma}{2}[e^{-(1+\alpha)\xi}+A(\xi)+B(\xi)]\left\{\frac{(1+\alpha)^2}{\alpha}\xi-e^{-\frac{(1+\alpha)^2}{\alpha}\xi}\sinh\left[\frac{(1+\alpha)^2}{\alpha}\xi\right]\right\}\right)/\left\{\frac{(1+\alpha)^4}{\alpha^2}\xi^2-\sinh^2\left[\frac{(1+\alpha)^2}{\alpha}\xi\right]\right\}, \tag{A4}$$

$$H(\xi)=\left(\frac{(1+\alpha)^2}{\alpha}\xi e^{(1+\alpha)\xi}-e^{\frac{(1+\alpha)}{\alpha}\xi}\sinh\left[\frac{(1+\alpha)^2}{\alpha}\xi\right]-\frac{\gamma}{2}[e^{-(1+\alpha)\xi}+A(\xi)+B(\xi)]\left\{\frac{(1+\alpha)^2}{\alpha}\xi-e^{\frac{(1+\alpha)^2}{\alpha}\xi}\sinh\left[\frac{(1+\alpha)^2}{\alpha}\xi\right]\right\}\right)/\left\{\frac{(1+\alpha)^4}{\alpha^2}\xi^2-\sinh^2\left[\frac{(1+\alpha)^2}{\alpha}\xi\right]\right\}, \tag{A5}$$

where

$$A(\xi)=\frac{\{\cosh[(1+\alpha)\beta\xi]\cosh[(1+\alpha)\xi]+\kappa\sinh[(1+\alpha)\beta\xi]\sinh[(1+\alpha)\xi]\}e^{-\frac{(1+\alpha)^2}{\alpha}\xi}}{\sinh\left[\frac{(1+\alpha)^2}{\alpha}\right]\xi\cosh[(1+\alpha)\beta\xi]+\kappa\cosh\left[\frac{(1+\alpha)^2}{\alpha}\xi\right]\sinh[(1+\alpha)\beta\xi]},$$

$$B(\xi)=\frac{\{-\cosh[(1+\alpha)\beta\xi]+\kappa\sinh[(1+\alpha)\beta\xi]\}\cosh\left[\left(\frac{1+\alpha}{\alpha}\right)\xi\right]}{\sinh\left[\frac{(1+\alpha)^2}{\alpha}\xi\right]\cosh[(1+\alpha)\beta\xi]+\kappa\cosh\left[\frac{(1+\alpha)^2}{\alpha}\xi\right]\sinh[(1+\alpha)\beta\xi]}.$$

References

Beck, F., 1981. Electrodeposition of paint. In: Bockris, J.O'M., Conway, B.E. Yeager, E., White, B.E., (Eds.). Comprehensive Treatise of Electrochemistry, Vol. 2 Electrochemical Processing. Plenum Press, New York.

Chen, S.B., Keh, H.J., 1988. Electrophoresis in a dilute dispersion of colloidal spheres. AIChE J. 34, 1075–1085.

Happel, J., Brenner, H., 1983. Low Reynolds Number Hydrodynamics. 3rd ed. Martinus Nijhoff, The Hague.

Haus, H.A., Melcher, J.R., 1989. Electromagnetic Fields and Energy. Prentice-Hall, Englewood Cliffs, NJ.

Hunter, R.J., 1981. Zeta Potential in Colloid Science. Academic Press, New York.

Ganatos, P., Weinbaum, S., Pfeffer, R., 1980. A strong interaction theory for the creeping motion of a sphere between plane parallel boundaries, part 1, Perpendicular motion. J. Fluid Mech 99, 739–753.

Gradshteyn, I.S., Ryzhik, I.M., 1994. Table of Integrals, Series and Products. 5th ed. Academic Press, New York.
Keh, H.J., Anderson, J.L., 1985. Boundary effects on electrophoretic motion of colloidal spheres. J. Fluid Mech. 153, 417–439.
Keh, H.J., Chen, S.B., 1988. Electrophoresis of a colloidal sphere parallel to a dielectric plane. J. Fluid Mech. 194, 377–390.
Keh, H.J., Jan, J.S., 1996. Boundary effects on diffusiophoresis and electrophoresis motion of a colloidal sphere to a plane wall. J. Colloid. Interface Sci. 183, 458–475.
Lamb, H., 1932. Hydrodynamics. 6th ed. Cambridge University Press, Cambridge.
Morrison, F.A., Jr, 1970. Electrophoresis of a particle of arbitrary shape. J. Colloid. Interface Sci. 34, 210–214.
Morrison, F.A., Jr, Stukel, J.J., 1970. Electrophoresis of an insulating sphere normal to a conducting plane. J. Colloid. Interface Sci. 33, 88–93.
Probstein, R.F., 1994. Physicochemical Hydrodynamics an Introduction. 2nd ed. Wiley, New York.
Reed, L.D., Morrison, F.A., Jr, 1976. Hydrodynamic interactions in electrophoresis. J. Colloid. Interface Sci. 54, 117–133.
Sneddon, I.N., 1951. Fourier Transforms. McGraw-Hill, New York.
Sonshine, R.M., Cox, R.G., Brenner, H., 1966. The Stokes translation of a particle of arbitrary shape along the axis of a circular cylinder. Appl. Sci. Res. 16, 273–300.